Miniature Antenna Enabling Near-field Eye-to-eye Communication in the MICS Band

Christoph Beck[1], Jörg Nagel[1], Christian Rusch[2], Georg Bretthauer[1]

Karlsruhe Institute of Technology (KIT)
[1]Institute of Applied Computer Science/Automation
[2]Institut für Hochfrequenztechnik und Elektronik

ABSTRACT

The Artificial Accommodation System (AAS) is a set of two tiny active medical implants meant to replace and imitate the natural eye lenses in case of cataract or presbyopia. The implants require a continuous exchange of sensor data between both eyes to determine the object distance. In this paper we present the design and characterization of a compact, differentially fed, multi-turn loop antenna for a near-field eye-to-eye communication link at 402–405 MHz (MICS). The bare antennas have a volume of just 1.1 mm^3 and exhibit a bandwidth of 5.6 %. The efficiency of the link was evaluated by 4-port measurements using a customized head phantom. The measured power transfer efficiency of −60.5 dB suggests the wireless link to be reliable and energy-efficient.

Categories and Subject Descriptors

J.3 [**Life and Medical Sciences**]: Medical information systems

General Terms

Desgin

Keywords

Artificial accommodation system, eye-to-eye communication, near-field, antenna design, planar loop, MICS, MedRadio

1. INTRODUCTION

Cataract and presbyopia are age-related phenomena that ultimately lead to a loss of accommodation, i.e. the eye loses its ability to focus on varying object distances. To restore accommodation after cataract treatment or in the case of presbyopia, the Artificial Accommodation System (AAS) is being developed [3]. The AAS is a small-sized active lens implant with a diameter of 10 mm meant to be implanted into the capsular bag of the eye, as depicted in Fig. 1. It consists of an active optical element in the implant center, a sensor system, a control unit, and an energy storage which will be recharged once a day or less frequently by means of an inductive link [11]. Additionally, a wireless eye-to-eye communication link between the two implants (distance $d = 65mm$ for an adult person) is required to determine the current object distance. As a communication standard, the Medical Implant Communication Service (MICS, also known as MedRadio) band at 402–405 MHz was chosen. It provides a good trade-off between high data rates and good signal propagation through body tissue. Furthermore, MICS is standardized by the ITU, has gained worldwide acceptance, and transceiver ICs are commercially available. While recent work primarily focused on the minimization of the communication duty cycle on the MAC (media access control) layer [1], this paper for the first time presents the progress in antenna development of the AAS.

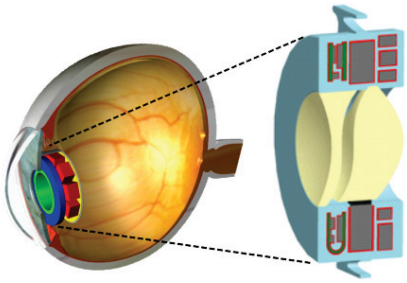

Figure 1: Schematic drawing of the Artificial Accommodation System (AAS) implanted into the capsular bag of the eye [14].

Due to severe space restrictions, existing MICS antennas cannot be adapted easily to fit into the AAS. Additionally, existing antennas are usually optimized with respect to their gain or radiation efficiency [10]. Such far-field properties are of minor importance to the application considered here. Since the near-field condition $d < \lambda/2\pi$ with λ being the wavelength at 402–405 MHz is satisfied [6], the antenna must instead be optimized in terms of its near-field power transfer efficiency. It is well known that the near-field of an electrically small loop antenna is dominated by magnetic field components [12]. As a result, the loop is less susceptible to detuning by the body compared to electrical antennas and absorption losses are smaller. Furthermore, loop antennas can be miniaturized very well by realizing multiple turns. For these reasons and because the shape of the AAS is ideally suited for a circular antenna, the (magnetic) loop was

BODYNETS 2013, September 30-October 02, Boston, United States

DOI 10.4108/icst.bodynets.2013.253508

chosen as antenna principle.

In this paper we present the design and evaluation of a compact multi-turn loop antenna for an inductive eye-to-eye communication link between two autonomous lens implants. Antenna design and simulation results are presented in Section 2. A capacitor-based matching method was applied to resonate the antenna in the MICS band when differentially driven by a 100 Ω transceiver (Section 3). Finally, measurement results of fabricated antennas in a body phantom environment are presented in Section 4. The results indicate that the proposed antenna is suited well for the given application.

2. ANTENNA DESIGN

The implant shape defines the maximum available area for the antenna. Since the inner part of the implant is occupied by the optics, the minimum and maximum radii of the antenna are 2.5 mm and 4.5 mm, respectively. A planar shape was chosen to occupy as little volume as possible and to be compatible with established thin film manufacturing processes. Besides the loop radius, the number of turns, n, the spacing between the turns, s, as well as the conductor width, w, can be adjusted. Because of the chosen fabrication process, the conductor height (9 μm) and substrate height (50 μm) are fixed. Although the exact interaction mechanisms among all parameters cannot be understood analytically, their qualitative effects will be summarized quickly: Both increasing radius and increasing number of turns boost the magnetic field of the antenna. However, they also increase ohmic losses and decrease the self-resonance frequency (SRF) of the loop. An increased conductor width lowers the resistance, hence increasing the Q factor. Finally, little spacing between the turns increases capacitive coupling between the turns and decreases the SRF.

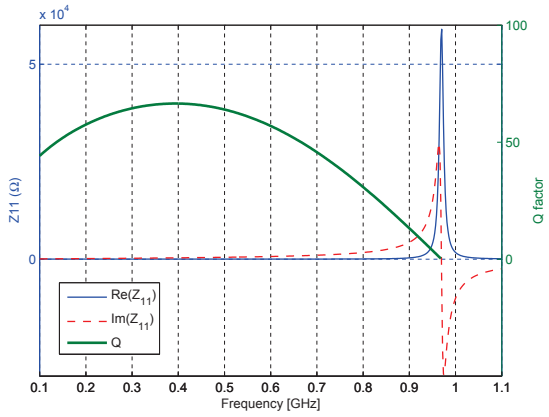

Figure 2: Q factor and impedance Z for the loop in free space for $n = 3$, $s = 200\mu m$, and $w = 50\mu m$.

The design goal is an optimization of the Q factor, which is defined as the ratio between stored magnetic energy in the near-field and the total dissipated energy. For inductors the common equation for Q, which is also adopted in this work, is $Q = \mathrm{Im}(Z)/\mathrm{Re}(Z)$, with Z being the complex impedance of the inductor or loop. Usually, the maximum Q is achieved well below the SRF [13]. A too high Q is disadvantageous

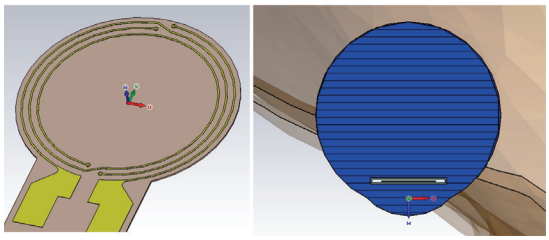

Figure 3: Left: Model of the symmetric loop with pads for feeding; Right: Geometry of the different simulation layers showing the antenna, encapsulation, eye and head tissue.

only in cases where losses are very small and bandwidth requirements would be violated as a result. However, this will not be the case for such a small-sized implanted antenna where additional losses arise due to high tissue conductivity.

We used CST Microwave Studio to determine the impedance and Q values of the loop as a function of the parameters mentioned above. For $n = 3$, $s = 200\mu m$, and $w = 50\mu m$, $Q = 66.5$ was maximum at the target frequency around 400 MHz in free space (Fig. 2). For simulations inside the body, the antenna was encapsulated by a 150 μm thick polyimide layer and was inserted 4.5 mm behind the cornea into the human eye (Fig. 3). Because the final implant design is still subject to changes, a 250 μm vacuum spacing between antenna and capsule was assumed to avoid direct shortening of the turns. Both eye and head were modeled homogeneously with relative permittivity and conductivity of 69.0/44.1 and $1.53\frac{S}{m}/0.87\frac{S}{m}$, respectively, at 400 MHz (compare Tab. 1). As expected, the SRF was lower in the lossy medium and decreased from 970 MHz to 833 MHz. The resistance increased significantly from 5.2 Ω to 9.1 Ω while the reactance just slightly increased from 342.9 Ω to 375.9 Ω.

3. MATCHING

The proposed antenna will be fed differentially to eliminate losses introduced by baluns and because of its better capability to reject common mode interference signals [15]. In a currently developed demonstration system of the AAS, the antenna will be connected to the Texas Instruments CC1101 transceiver with a differential input/output resistance of roughly 100 Ω at 400 MHz [16]. Thus, for the matched antenna, $Z_M = 100\Omega$ shall be the target impedance.

A very simple and space-saving method to match the antenna while keeping its symmetry is to add a capacitor in series with each leg of the antenna (C_S) and an additional capacitor as shunt element (parallel capacitor C_P) between the feeding points (Fig. 4). The shunt element transforms the resistance to the desired value while the series elements compensate for the resulting reactive part of impedance. Since the combination of loop inductance and series capacitors still yields a positive reactance, the matching circuit can be considered an L network [4].

To determine ideal capacitor values, we first transformed the differential network to an equivalent single-ended network as described in [15]. Based on the results, the commercially available capacitors $C_P = 12pF$ and $C_S = 2.4pF$ were chosen. Figure 5 depicts the simulation results of the matched antenna in free space and inside the body. The

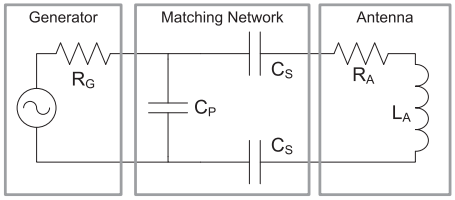

Figure 4: Differential matching of the antenna with three capacitors. The antenna is represented by the loop inductance in series with a resistor summarizing ohmic, radiation, and dielectric losses.

capacitors were modeled as lumped elements with an equivalent series resistance (ESR) of 0.1 Ω. It can be seen that the reflection is lowest inside the body environment and the resonance frequency drops by about 15 MHz compared to free space conditions.

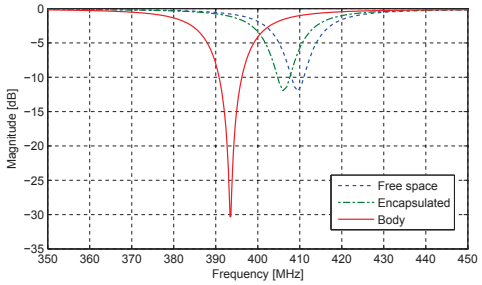

Figure 5: Simulated S11 parameters of the matched antenna in free space, polyimide housing, and inside the head model.

4. RESULTS

4.1 Measurement Setup

Several antennas ($n = 3$, $s = 200\mu m$, $w = 50\mu m$) were fabricated on flexprint circuit boards as shown in Fig. 6. The 50 μm thick substrate is based on DuPont Pyralux AP (polyimide) and the metallization was TiW/Au/Ni/Au with a total height of 9 μm. The area and volume required for the bare antenna (excluding matching capacitors, solder pads, and the inner cylinder that will accommodate the optics later) are 17.2 mm^2 and 1.1 mm^3, respectively.

The pins of each antenna were soldered to a measurement fixture made of two semirigid cables with a length of 70 mm to connect the antennas to a vector network analyzer (VNA). The VNA used was the Agilent PNA-X N5247A where all available four ports were employed to measure differential reflection and transmission coefficients. In other words, two physical ports of the VNA yield one logical port. According to the theory of mixed-mode S-parameters [5], the differential (or odd mode) reflection coefficient, S_{dd11}, is calculated as $S_{dd11} = \frac{1}{2}(S_{11} - S_{12} - S_{21} + S_{22})$ with S_{ij} being the single-ended reflection and transmission coefficients referring to the physical ports i and j. For a symmetric device, $S_{22} = S_{11}$ and $S_{21} = S_{12}$ [17] and we obtain

$$S_{dd11} = S_{11} - S_{21}. \quad (1)$$

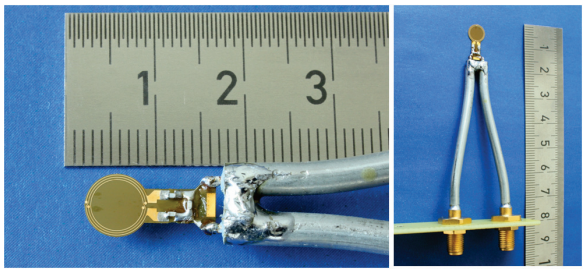

Figure 6: Matched antenna with fixture for measurements.

Likewise, the differential transmission coefficient, S_{dd21}, of two symmetric devices ($S_{31} = S_{42}$ and $S_{32} = S_{41}$ due to symmetry) is calculated as

$$S_{dd21} = S_{31} - S_{41} = \eta = P_R/R_T. \quad (2)$$

S_{dd21} directly gives the power transfer efficiency (i.e. negative path loss), η, of the two antennas where P_T is the transmitter and P_R the receiver power. The employed VNA is capable of automatically deriving the mixed-mode S-parameters from single-ended port measurements.

4.2 Head Phantom

The antennas were evaluated in a customized head phantom [2] that is shown in Fig. 7. The phantom consists of a polymer head shell filled with a head tissue-mimicking fluid. The eyes are made of a 10 % gelatin solution. The permittivity and conductivity values of both head and eye materials were adjusted by adding salt and sucrose. The material composition and dielectric properties are summarized in Table 1.

Table 1: Composition and dielectric properties of the head- and eye-equivalent materials. The target values from literature are given in brackets.

	Head material	Eye material
Composition	Water 40.2 wt%	Water 89.2 wt%
	Sugar 56.3 wt%	Gelatin 10.0 wt%
	NaCl 3.5 wt%	NaCl 0.8 wt%
ϵ_r	47.6 (44.1 [9])	69.7 (69.0 [7])
$\sigma[S/m]$	0.84 (0.87 [9])	1.41 (1.53 [7])

4.3 Measurement Results

In analogy to the simulations, the antennas were characterized with and without encapsulation in free space and inside the head phantom. Both the differential reflection coefficients S_{dd11}/S_{dd22} and the path loss S_{dd21} were measured. For simplicity, the subscripts dd are omitted. Fig. 8 depicts the results. For reasons of clarity, the curves for the encapsulated antenna in free space are not shown. However, it may be noted that the measurement results of the antenna with and without encapsulation in free space are very similar. It can be seen that the simulation and measurement results agree well, although the measured resonance frequency is a few MHz lower and the antenna bandwidth is a few percent higher than simulated. Our explanation is that the real losses are higher than expected, e.g. due to tolerances in the fabrication process, solder joints or a higher

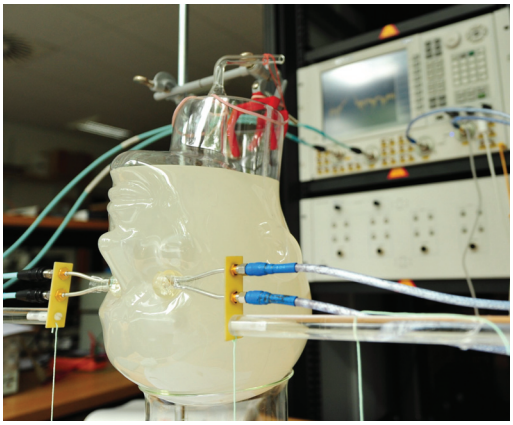

Figure 7: Experimental setup showing the head phantom, antennas and the 4-port NVA.

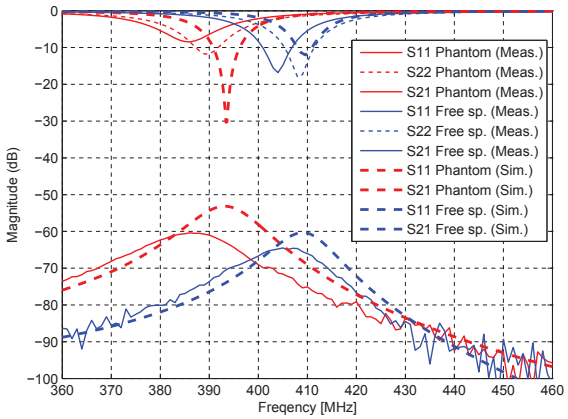

Figure 8: Comparison between measured and simulated S11- and S21-parameters

ESR of the capacitors than assumed. This would explain the higher bandwidth due to a lower Q and the fact that the real antennas are better matched in free space than in the head phantom.

From Fig. 8 it can also be seen that the path loss is lower inside the body than in free space for both simulations and measurements. This is remarkable since the body introduces additional losses and (at least for the real experiments) the antenna matching was poorer. However, the effect of enhanced magnetic fields close to the body surface were also observed in other applications [8]. Considering the small size of the antennas, the measured path loss of 60.5 dB inside the body is acceptable. Assuming a receiver sensitivity of -95 dBm, a required SNR of 10 dB, and an additional loss of 10 dB due to antenna mismatch and coil misalignments, a minimum transmit power of -15 dBm would be required for the eye-to-eye communication link of the AAS.

5. CONCLUSIONS

We proposed a miniature antenna for the near-field eye-to-eye communication link of a novel lens implant system. The antenna is based on a planar multi-turn loop matched for differential feeding in the MICS band. A pair of antennas was characterized inside a customized head phantom using 4-port measurements to derive differential reflection coefficients and the power transfer efficiency of the communication link. The achieved bandwidth of 5.6 % and power transfer efficiency of −60.5 dB show that the antenna is suited well for application in the AAS.

6. ACKNOWLEDGMENTS

Thanks to M. Jalilvand and the entire Institut für Hochfrequenztechnik und Elektronik (IHE) at KIT for measurement equipment and assisting in the characterization process.

7. REFERENCES

[1] C. Beck, P. Hevesi, J. Nagel, G. Bretthauer, and R. Guthoff. A cyclic MAC layer synchronisation approach for time-critical low-power body sensor networks. In *IEEE PIMRC '11, Toronto, Canada*, Sept. 2011.

[2] C. Beck, S. Nägele, J. Nagel, H. Guth, U. Gengenbach, and G. Bretthauer. Low-cost head phantom for the evaluation and optimization of RF-links in ophthalmic implants. In *BMT 2013, Graz, Austria*, 2013. (Accepted Paper).

[3] G. Bretthauer, U. Gengenbach, and R. Guthoff. The Artificial Accommodation System – A mechatronic implant for restoration of accommodation. In *Biomed. Technik / Biomedical Engineering*, volume 55(Suppl. 1), 2010.

[4] L. Burgess. Matching RFIC wireless transmitters to small antennas. *HF Electronics*, p 20–28, march 2005.

[5] W. Fan, A. Lu, L. Wai, and B. Lok. Mixed-mode S-parameter characterization of differential structures. In *EPTC 2003*, 2003.

[6] K. Fotopoulou and B. Flynn. Wireless power transfer in loosely coupled links: Coil misalignment model. *IEEE Transactions on Magnetics*, 47(2):416–430, Feb. 2011.

[7] S. Gabriel, R. W. Lau, and C. Gabriel. The dielectric properties of biological tissues. *Physics in Medicine and Biology*, 41(11):2251, 1996.

[8] P. S. Hall and Y. Hao. *Antennas and Propagation for Body-Centric Wireless Communications*. 2006.

[9] *IEEE Std 1528-2003*, 2003.

[10] F. Merli, L. Bolomey, J.-F. Zurcher, G. Corradini, E. Meurville, and A. K. Skrivervik. Design, realization and measurements of a miniature antenna for implantable wireless communication systems. *IEEE Trans. on Antennas and Propagation*, 59(10):3544–3555, October 2011.

[11] J. Nagel, M. Krug, U. Gengenbach, H. Guth, G. Bretthauer, and R. F. Guthoff. Optimal secondary coil design for inductive powering of the artificial accommodation system. In *EMBC '11*, 2011.

[12] M. Norris, J.-D. Richerd, and D. Raynes. Sub miniature antenna design for wireless implants. In *Antennas and Propagation for Body-Centric Wireless Communications, 2007 IET Seminar on*, pages 57–62, april 2007.

[13] S. J. Pan, W.-Y. Yin, and J. L.-W. Li. Performance trends of on-chip spiral inductors for RFICs. *Progress In Electromagnetics Research*, 45:123–151, 2004.

[14] L. Rheinschmitt. *Erstmaliger Gesamtentwurf und Realisierung der Systemintegration für das Künstliche Akkommodationssystem*. Dissertation, Fakultät für Maschinenbau, Universität Karlsruhe, 2011.

[15] Skyworks. *Matching Differential Port Devices*, 2009.

[16] Texas Instruments. CC1101 low-power sub-1 GHz RF transceiver, 2010.

[17] H. Zhu, Y. Ko, and T. Ye. Impedance measurement for balanced UHF RFID tag antennas. In *Radio and Wireless Symposium (RWS), 2010 IEEE*, 2010.